Thresholds of fire response to moisture and fuel load differ between tropical savannas and grasslands across continents

Swanni T. Alvarado, Niels Andela, Thiago S. F. Silva, Sally Archibald

Short running title: Tropical savanna climate-fire responses

Abstract

Aim: An emerging framework for tropical ecosystems states that fire activity is either '*fuel build-up limited*' or '*fuel moisture limited*' i.e. as you move up along rainfall gradients, the major control on fire occurrence switches from being the amount of fuel, to the moisture content of the fuel. Here we used remotely sensed datasets to assess whether interannual variability of burned area is better explained by annual rainfall totals driving fuel build-up, or by dry season rainfall driving fuel moisture.

Location: Pantropical savannas and grasslands

Time period: 2002-2016

Methods: We explored the response of annual burned area to interannual variability in rainfall. We compared several linear models to understand how *fuel moisture* and *fuel build-up effect* (accumulated rainfall during 6 and 24 months prior to the end of the burning season respectively) determine the interannual variability of burned area and explore if tree cover, dry season duration and human activity modified these relationships.

Results: Fuel and moisture controls on fire occurrence in tropical savannas varied across continents. Only 24% of South American savannas were *fuel build-up limited* against 61% of Australian savannas and 47% of African savannas. On average, South America switched from fuel limited to moisture limited at 500 mm yr^{-1}, Africa at 800 mm yr^{-1} and Australia at 1000 mm yr^{-1} of mean annual rainfall.

Main conclusions: In 42% of tropical savannas (accounting for 41% of current area burned) increased drought and higher temperatures will not increase fire, but there are savannas, particularly in South America, that are likely to become more flammable with increasing temperatures. These findings highlight that we cannot transfer knowledge of fire responses to global change across ecosystems/regions – local solutions to local fire management issues are required, and different tropical savanna regions may show contrasting responses to the same drivers of global change.

Keywords: tropical savannas, fire regimes, fuel build-up, fuel moisture, ecosystem models, future scenarios

1. Introduction

Understanding global controls on fire activity has become increasingly important in the context of ecosystem drying and climatic change (Jolly et al., 2015). In some ecosystems drought events and rising temperatures may exacerbate fire risk (Bowman et al., 2011; Price et al., 2015), and increase the incidence of large wildfires and fire-associated CO_2 emissions (Voulgarakis & Field, 2015; Hantson *et al.*, 2017). However, not all ecosystems burn more when exposed to drought and high temperatures. Pausas and Ribeiro (2013) showed that fire in lower-productivity systems was unresponsive to temperature, and paleo-records highlight regional differences in fire responses to changes in rainfall and temperature (Daniau *et al.*, 2012). Bradstock (2010) indicated that fire would respond to the factor that was most limiting in a particular ecosystem – and when there is no fuel to burn increased temperatures and drought conditions would be expected to have little impact on fire. Fires are therefore the outcome of complex interactions between climate, fire, vegetation and land management (Moritz *et al.*, 2012; Andela *et al.*, 2017; Forkel *et al.*, 2017; Abatzoglou *et al.*, 2018). Fire enabled Dynamic Global Vegetation Models (DGVMs) are designed to model these interactions, but model outcomes vary widely across models (Bowman *et al.*, 2014; Williams & Abatzoglou, 2016; van Marle *et al.*, 2017), based on a wide range of different parameterizations (Hantson *et al.*, 2016; Rabin *et al.*, 2017). The role of fire for carbon cycling and maintaining biodiversity under scenarios of future change therefore remain uncertain for tropical biomes.

Fire is an essential ecosystem process in tropical savannas and grasslands, which are characterized by high fire frequency under natural conditions (Bond *et al.*, 2005; Chuvieco *et al.*, 2008). Rainfall is the dominant control on fire activity in the tropics (van der Werf *et al.*, 2008); seasonal variation in tropical savanna rainfall typically results in vegetation production and biomass build-up during the wet season, followed by a dry period when dead or dormant herbaceous vegetation becomes flammable (Bradstock, 2010). The dynamic balance of productivity and seasonal drought also determines the interannual variability of burned area (Pausas & Ribeiro, 2013). In the humid tropics fire activity is constrained by fuel moisture conditions (*fuel moisture limited*) (Bradstock, 2010; Whitlock *et al.*, 2010): here negative rainfall anomalies increase fire activity by causing usually green, non-flammable vegetation to dry out sufficiently to carry fire (Aragão *et al.*, 2008). In contrast, in tropical biomes with low net primary productivity such as grasslands and xeric savannas, fire activity is constrained by fuel produced during the preceding growing seasons (*fuel build-up limited*)

(Whitlock *et al.*, 2010; O'Donnell *et al.*, 2011; Kahiu & Hanan, 2018): here anomalous wet years increase vegetation productivity which increases fire activity during the following dry seasons (Van Wilgen *et al.*, 2004; Archibald *et al.*, 2010; Pausas & Paula, 2012; Abatzoglou *et al.*, 2018).

Despite the important differences in fire ecology and behavior across fuel and moisture limited fire regimes, their global distribution remains unknown. While climate determines where and when fires can occur (van der Werf *et al.*, 2008; Archibald *et al.*, 2010), human land management modifies regional patterns of fire activity (Bistinas *et al.*, 2013; Andela *et al.*, 2017). Humans are a source of ignitions as fire is often used as a tool in pastoral and agricultural activities (Mistry, 2000; Cochrane & Ryan, 2009), but humans also alter fire sizes by increasing landscape fragmentation and changing the timing of ignitions (Le Page *et al.*, 2010). Moreover, there is evidence that the sensitivity of fire regimes to climate variability depends on human activities (Archibald *et al.*, 2010), as humans can "buffer" ecosystems (Bird *et al.*, 2012) from climate and fire extremes through the way that they manage landscapes and light fires (Yibarbuk *et al.*, 2002; Price *et al.*, 2012; Bird *et al.*, 2016). Vegetation cover and type also interact with fire, as grasses produce fine fuels that carry savanna fires. Tree cover in turn, may reduce fire occurrence by limiting grass productivity (Bond *et al.*, 2005; Hoffmann *et al.*, 2012; Aleman & Staver, 2018). The effects of climate and human land management on fire activity are therefore further modified by vegetation type, its cover and productivity (Archibald *et al.*, 2009; Bistinas *et al.*, 2014; Lehmann *et al.*, 2014).

Here we use satellite observations to study burned area-rainfall relationships across a moisture gradient, ranging from xeric grasslands to mesic tropical savannas. First, we identify pantropical rainfall thresholds where savanna and grassland fire regimes switch from *fuel build-up limited* to *fuel moisture limited*. Second, we investigate how these thresholds vary across regions and how spatial patterns in *fuel build-up-* and *fuel moisture limited* fire regimes are modified by rainfall seasonality, human activity, and tree cover. Understanding how climate, human activity, and ecosystem structure modify the response of fire activity to changing weather conditions is critical to model and forecast future fire activity across different environments.

2. Data and methods

2.1. Remote sensing data

For our analysis, we rescaled all data to 0.25° spatial resolution by calculating the mean value, land cover type formed a notable exception as we used the dominant cover type within each larger 0.25° grid cell.

Savanna and grassland cover. We used the Moderate Resolution Imaging Spectroradiometer (MODIS) Global Land Cover product (MCD12C1 collection 5.1) for 2012 (Friedl *et al.*, 2010) to delimit savanna and grassland extent across continents. We included all 0.25° grid cells (25°N - 25°S) where savannas and grasslands formed the dominant land cover type, based on the combined cover of "woody savannas", "savannas", and "grasslands" according to the International Geosphere-Biosphere Programme (IGBP) classification. We focus on "natural lands", by excluding croplands and urban areas from our analysis, because we expect that fuel-build up and moisture status would primarily depend on management practice instead of antecedent rainfall across these landscapes. In addition, we used the MODIS vegetation continuous fields product (MOD44B collection 5 for 2010, (DiMiceli *et al.*, 2011) to exclude areas with tree cover > 40%, assuming that savannas with high tree cover are less flammable (Archibald *et al.*, 2009), and because fires are difficult to detect under canopies (Morton *et al.*, 2011). In this study we analyzed data from Africa (55.6%), Australia (7.8%) and South America (27.4%), together containing 90.8% of the delimited tropical savannas and grasslands. Tropical savannas in Asia (6.1%) and Central America (3.1%) are highly fragmented and poorly defined (e.g., Ratnam *et al.*, 2016), and were therefore excluded from our analysis.

Burned area data. We derived the percentage of monthly burned area per 0.25° grid cell from the MODIS MCD64A1 collection 6 global burned area product (Giglio *et al.*, 2018). Subsequently, we derived time series of annual burned area (BA in % yr^{-1}) per fire year for each 0.25° grid cell for 2002–2016. For each grid cell, we delimited the fire-year as the 12-month period centered on the month of maximum mean burned area (from 5 months before to 6 months after the month of maximum burned area). This step is required because in the northern hemisphere tropics the fire season typically includes months of two calendar years, with maximum fire activity occurring in December or January. Based on these fire years, we defined the start and end months of the burning season as the all-year mean month where 10% and 90% of annual burned area had occurred, respectively. Our analysis is based on the assumption of clear seasonality with a unique fire season per year, which is generally true across tropical grasslands and savannas (Benali *et al.*, 2017).

Burned area drivers. Monthly rainfall data were obtained from the Climate Hazards Group InfraRed Precipitation with Station (CHIRPS) dataset (Funk *et al.*, 2015) for the extended study period between 2002–2016. We used rainfall data to calculate mean annual rainfall (MAR, in mm yr^{-1}, Fig 1b) over the calendar year and estimate the *fuel moisture* and *fuel build-up effects* on interannual variability in burned area. We defined the *fuel moisture effect* as the accumulated rainfall during the six months prior to the end of the burning season. We assumed that rainfall occurring during, or just before the burning season determines the probability of ignition and fire spread. The *fuel build-up effect* was defined as the accumulated rainfall during 24 months prior to the end of the burning season, as previous rainfall is an important control on the amount of biomass produced. We selected the 6- and 24-months cut-off as, on average, the strongest negative response in *fuel moisture limited* landscapes was found around 6-7 months of antecedent rainfall (Fig. A1), while across *fuel build-up limited* landscapes accumulated rainfall over two wet seasons (24-months) had a slightly higher explanatory power than over a single wet season (12-months) (Fig. A1).

We considered three explanatory variables for our initial analysis of the drivers of observed spatial patterns in *fuel build-up* and *fuel moisture limited* fire regimes. First, we focus on spatial differences in dry season duration. Following Hulme & Viner (1998), we define the dry season duration (in months) as the average number of months with rainfall below 50 mm $month^{-1}$ during the 2002 – 2016 calendar years (Fig. A2b). This intermediate (50 mm $month^{-1}$) rainfall threshold assures reasonable sensitivity to dry season duration across both arid and more humid tropical environments. Second, to investigate how humans affect fire occurrence and climate-fire interactions, we used the Wildlife and Conservation Society (WCS) Human Influence Index (HII, Fig. A2a) (WCS & University, 2005), a measure, varying between 0 and 64 (for no human and maximum influence respectively), of the direct human influence on ecosystems based on eight different measures of human presence: population density (people per km^2), land cover type, and a measure of the presence of railroads, major roads, navigable rivers, coastlines, nighttime stable lights, and urban polygons. Third, because vegetation structure can affect fire activity and varies across continents (Lasslop *et al.*, 2018), we also considered tree cover as an explanatory variable for observed patterns of *fuel* and *moisture limited* fire regimes. Tree cover data was obtained from MODIS vegetation continuous fields (MOD44B collection 5, Fig. A2c) for 2010 (DiMiceli et al., 2011). Because in our definition of tropical savannas and grasslands we already excluded areas with tree cover >40%, this variable ranged from 0 to 40%.

166 ## 2.2. Methods

167 **Burned area response to *fuel moisture* and *fuel build-up effects***. Based on the per-fire-year
168 burned area time series, we explored the response of annual burned area to interannual
169 variability in rainfall for each 0.25° grid cell. All grid cells that showed negative correlations
170 (Pearson's r) between antecedent rainfall accumulated over 6 months prior to the end of the
171 burning season and annual BA were considered *fuel moisture limited* fire regimes, indicating
172 higher burned area when accumulated rainfall was low during or shortly before the burning
173 season. Similarly, we considered ecosystems to be *fuel build-up limited*, for all grid cells with
174 a positive correlation between annual BA and antecedent rainfall accumulated during 24
175 months prior to the end of the burning season. Some grid cells had both negative correlations
176 (*fuel moisture effect*) with the short lead times and positive correlations (*fuel build-up effect*)
177 with the long lead times, but in these cases, effects were generally not significant at the same
178 time ($p<0.05$ in 5% of total grid cells). For simplicity, we therefore selected the strongest
179 absolute correlation for each grid cell.

180 Based on the biome wide characterization of burned area response to antecedent rainfall,
181 we explored how these relationships varied across continents. First, we identified the MAR
182 threshold where fire regimes switched from being *fuel build-up limited* to being *fuel moisture*
183 *limited*. We binned the per grid cell strongest absolute (i.e. positive or negative) correlation
184 between annual BA and antecedent rainfall into 100 mm MAR bins. We then defined the
185 threshold where ecosystems switched from *fuel build-up limited* to *fuel moisture limited* (and
186 vice versa) as the MAR bin where >50% of the correlation coefficients switched from
187 negative to positive (i.e. the median value in a boxplot crossed the zero line).

188 **Drivers of burned area response.** We used two different approaches to explore the drivers
189 of spatial differences in the relationship between annual burned area and antecedent rainfall.
190 First, to keep annual rainfall constant, we binned all grid cells based on 200 mm yr^{-1} MAR
191 increments; within each rainfall bin, we further subdivided the grid cells based on bins of dry
192 season duration (DS; increments of months with rainfall below 50 mm), Human Influence
193 Index (HII; increments of 5 units of HII, HII ranged from 0 to 40 across the study area), and
194 tree cover (TC; 5% increments from 0 to 40%). Based on this subdivision along rainfall
195 gradients, we explored how DS, HII, and TC modified patterns of a) mean annual burned
196 area, b) interannual variability in burned area (measured as the coefficient of variation), and c)
197 the correlation coefficient between antecedent rainfall and annual BA.

Second, we compared two multiple linear regression models to understand how the *fuel moisture effect* (Rain6, 6 months of accumulated rainfall) and the *fuel build-up effect* (Rain24, 24 months of accumulated rainfall) influenced the interannual variability of BA (Eq. 1) and investigate if BA response to rainfall varied at continental scales (Eq. 2). In order to increase model sensitivity to temporal variability in burned area, we used burned area anomalies rather than absolute burned area time series.

$$BA_{i,j}\ \text{anomaly} \sim \alpha + \beta_1 * Rain6_{i,j} + \beta_2 * Rain24_{i,j} + \varepsilon \qquad \text{Equation 1}$$

$$BA_{i,j}\ \text{anomaly} \sim \alpha + \beta_1 * Rain6_{i,j} : \text{Continent} + \beta_2 * Rain24_{i,j,t} : \text{Continent} + \varepsilon \qquad \text{Equation 2}$$

where $BA_{i,j}$ anomaly is the burned area anomaly for each pixel (i) and year (j) calculated as $BA_{i,j}$ – mean BA_i, β parameters represent the slope of the linear regression between the BA anomaly and the explanatory variables ($Rain6_{i,j}$ and $Rain24_{i,j}$), α is the intercept and ε the residual error term. The BA anomaly includes both negative and positive values, where negative values indicate that the BA for the year *j* was lower than the mean BA and positive values indicate that annual BA was higher than the mean. Thus, β_1 and β_2 indicate the rate of BA change per unit of accumulated rainfall (% $year^{-1}$ mm^{-1}).

Next, we explored how other variables, including MAR, DS, HII and/or TC modify the influence of antecedent rainfall on burned area anomalies by analyzing how the β_1 and β_2 values changed when introducing each driver in the model. In addition, when including a new variable, we compared the model with and without the effect in question, using an ANOVA likelihood-ratio test and AIC (Akaike's Information Criterion) to confirm the selection of the best model (Burnham & Anderson, 2004). Finally, we constructed the same models, but now based on full burned area time series instead of anomalies. This analysis helped to understand how each variable contributes to both spatial and temporal patterns of biome wide burned area. All analyses were done using the 'raster' and 'rgdal' packages in R, version R2.5.1 (R Core Team, 2016).

3. Results

3.1. Burned area response to antecedent rainfall

We observed the strongest correlations between antecedent rainfall and annual burned area (BA) in frequently burning savannas and grasslands across the tropics (Fig. 1). Here we considered grid cells with a negative correlation between burned area and rainfall (6-month lead time) to be *fuel moisture limited* and grid cells with a positive correlation (24-month lead

time) to be *fuel build-up limited*. Interestingly, we found that savannas with *fuel build-up limited* fire regimes (41.4%) in more arid regions covered less area than savannas with *fuel moisture limited* fire regimes (58.6%, Fig. 1b, e) in more humid systems. Mean annual rainfall (MAR) varied widely across tropical savannas on the three continents, resulting in predominantly *fuel moisture limited* fire regimes across the relatively humid savannas of South America, and *fuel build-up limited* fire regimes across Australian savannas that were more arid on average (Fig. 1b to 1e). Africa showed a mix of *fuel* and *moisture limited* savannas across a large rainfall gradient. For example, we observed strong positive correlations for arid regions (e.g. Namibia, Botswana and Zimbabwe) and strong negative correlations for humid regions (e.g. the north of Mozambique and the south of Tanzania and the Democratic Republic of Congo) (Fig. 1e).

3.2. Continental differences in the switch from fuel build-up to fuel moisture limitation

Africa tropical savanna and grassland fire regimes switched from a predominantly positive (*fuel build-up effect*) to negative (*fuel moisture effect*) response to antecedent rainfall around 800 mm annual rainfall (Fig. 2), while fire regimes in South America switched around 500 mm yr^{-1}, and in Australia around 1000 mm yr^{-1} (Fig. 2). For all three continents, MAR bins that contained a low number of grid cells often showed a more variable response (cf. Figs. 2 and A3). We also observed large spatial variability in burned area-rainfall responses (Fig. 1 and 2), indicating that the switch from *fuel build-up* to *fuel moisture limited* fire regimes occurred gradually. On each continent, there was a transition zone in MAR levels rather than a clear threshold, where the strength of the dominant correlation weakened before switching to a different dominant driver. Only 24% of South American savannas were *fuel build-up limited* against 61% of Australian savannas and 47% of African savannas.

3.3.Drivers of continental differences.

In addition to MAR, we explored how rainfall seasonality influences median annual BA and interannual variability in BA, both important indicators of the strength of fire-climate interactions. Globally, longer dry season durations tended to increase median annual BA, particularly in intermediate productive savannas and grasslands (MAR between 900-1500 mm, Fig 3a). Interestingly, when dry season length exceeded 9 months, annual burned area typically declined again, likely because very short growing seasons may limit ecosystem productivity and thus fuel availability. In addition to burned area, we also analyzed its coefficient of variation, we hypothesize that the strength of the burned area response to

antecedent rainfall partly depends on the variability of both variables. For bins of comparable rainfall and dry season duration, Australia showed the lowest coefficients of variation, potentially weakening correlation coefficients between antecedent rainfall and burned area, seen as a more variable response of positive and negative correlations (Fig 3b and c). In contrast, large on average coefficients of variation across South America may be responsible for the relatively strong negative correlation observed across productive savannas. We also observed a reduction in the coefficient of variation in areas of high fraction of annual burned area (Fig. 3b), possibly reducing the strength of the correlation between annual burned area and fuel conditions (Fig. 3c). Although dry season duration clearly affected burned area and it's variability, patterns were not uniform, suggesting other factors also played a role.

Human impact strongly reduced burned area across continents (Fig. 4a), while Australian savannas and grasslands were generally characterized by low human impact values (HII <10) and African and South American savannas were characterized by higher impact values (HII = 10-25; Fig. 4b). The coefficient of variation was clearly reduced in natural areas with a large fraction of burned area and low human influence (Fig. 4b). Despite the large impact of HII on absolute burned area, impacts on the interannual variability were more limited and complex. Globally, a small decline in the strength of the burned area response to rainfall variability was observed with decreasing HII and increasing burned area in the peak biomass burning regions (MAR ranging from 900 – 1500 mm yr^{-1}; Fig. 4c). In contrast, at continental scales sometimes the opposite pattern was observed. For example, in productive savannas (MAR 1300 – 2100 mm yr^{-1}) of South America the negative correlation between antecedent rainfall and burned area strengthened with decreasing HII. The global pattern in the response of BA to the *fuel build-up* and *fuel moisture effects* was mainly determined by South America and Africa, with a dominant negative response in savannas with MAR above 900 mm yr^{-1} and positive response in savannas with MAR below 900 mm yr^{-1}, independently of the HII (Fig. 4c).

Vegetation structure also influenced biome wide patterns of burned area and the strength and sign of correlation coefficients between antecedent rainfall and burned area (Fig. 5). As expected, we observed that higher tree cover was often associated with reduced burned area, particularly in the humid tropics (Fig. 5a). In productive savannas (MAR ranging from 900 to 2000 mm yr-1), the fuel moisture effect tended to strengthen with increasing tree cover, although relationships were often weak (Fig. 5c). In fuel limited ecosystems of Australia, there was a weak increase in the strength of the fuel build-up effect with tree cover, opposite to the global pattern, where the strength of the fuel build-up effect weakened with increasing

tree cover. As noted earlier, coefficients of variation varied widely across continents, possibly strengthening or weakening regional correlation coefficients. In contrast to Africa and Australia, South America showed high coefficients of variation for savannas of intermediate productivity, likely contributing to the exceptionally strong moisture limitation on regional burned area.

Despite the clear biome wide patterns of *fuel moisture* and *fuel build-up limited* fire regimes, we could not establish a single global model to explain the interannual variability in burned area (BA) based on *fuel build-up effect* and *fuel moisture effect* alone (Table 1). Here we used multiple linear regression models to test the effect of the antecedent rainfall on BA anomalies (Table 1) per pixel across the time series, and the spatial and temporal pattern in BA time series (Table A1), across tropical savannas and grasslands. We expect that the model based on BA anomalies is better able to capture interannual variability, while the second model captures both temporal variability and spatial patterns of burned area. The global model of BA anomalies that included only the *fuel build-up effect* and *fuel moisture effect* as explanatory variables explained less than 1% of BA variation (Table 1), while the same model for absolute BA explained 3% of the variance (Table A1). Surprisingly, BA did not vary as expected when an interaction term between MAR and *fuel build-up effect* and *fuel moisture effect* was added to the model and its performance did not improve. In contrast, the inclusion of "continent" as an interaction term with the 6- and 24-month accumulated rainfall increased the percent of explained variance and reduced AIC for both BA (from 3.6 to 19%, Table A1) and its internannual variability (from 0.0019 to 0.0029%, Table1). Both models, supported different slopes between the *fuel moisture effect* and *fuel build-up effect* and burned area across continents ($p < 0.001$), confirming continental scale differences in burned area-rainfall response (Table 1 and A1, Fig. 2).

The models with the highest explanatory power (lowest AIC) explained 0.4% of the variance of the interannual variability of BA (Table 1) and 29% of spatial occurrence (Table A1). These models included *tree cover*, *dry season duration* and *HII* all in interaction with *Continent* as additional factors to *fuel build-up effect* and *fuel moisture effect.* The response of BA anomalies to the *fuel-moisture effect* and the *fuel build-up effect* was strongest in Australia (β_1 = -0.0036 % mm^{-1} and β_2 = 0.0019 % mm^{-1} respectively, Table 1) and weakest in Africa (β_1 = -0.0012 % mm^{-1} and β_2 =0.00035 % mm^{-1} respectively, Table 1). Statistical analysis confirmed the expected response, with negative slope coefficients for *fuel moisture effect* and positive coefficients for *fuel build-up effect* (Table 1). The inclusion of *tree cover*, *dry season*

duration or *HII* in the models modified the slopes of *fuel build-up effect* across all the three continents, while the slopes for *fuel moisture effect* remained more similar (Table 1). When we included all three variables in the model, we detected a slight decrease in the slope of *fuel build-up effect* for African (from 0.00041 to 0.00035% mm^{-1}) and South America savannas (from 0.00058 to 0.00046% mm^{-1}) and a larger increase for Australian savannas (from 0.00088 to 0.0019% mm^{-1}, Table 1). The inclusion of these three factors also modified the intercept sign from negative to positive indicating a positive anomaly (BA > mean BA) when these factors are zero. When considering the inclusion of each of these explanatory variables (DS, HII, and TC) separately, the inclusion of dry seasons length had the strongest effect on the response of BA to the *fuel build-up effect;* in Africa β_2 decreased from 0.00041 to 0.00023% mm^{-1} and the smallest effect was observed in South America from 0.00058 to 0.00051 % mm^{-1}. In contrast, the inclusion of HII had the strongest effect on the response of BA to the *fuel build-up effect* in Australia $\beta_{2,}$ increasing from 0.00088 to 0.0011% mm^{-1} while in Africa and South America we observed a slight decrease (from 0.00041 to 0.00040% mm^{-1} and from 0.00058 to 0.00054% mm^{-1} respectively). The inclusion of tree cover had the strongest effect on the response of BA to the *fuel build-up effect* for South America, β_2 increased from 0.00058 to 0.010% mm-1. When we analyzed the absolute BA (Table A1), HII coefficients were also negative for the three continents, in line with lower burned area in human dominated landscapes (Archibald *et al.*, 2012; Andela *et al.*, 2017), with the highest decrease in BA variation when human influence increased in Australia (β_4 = -3.10%), and a similar lower variation observed in Africa and South America (β_4 = -1.29% and -1.10% respectively, Table A1).

4. Discussion

4.1. Fire-climate threshold

Here we explore the extent of *fuel build-up* and *fuel moisture limited* fire regimes across tropical savannas based on a per-pixel temporal correlation between burned area and antecedent rainfall. Savanna fire-climate interactions changed along gradients of mean annual precipitation, with burned area in xeric savannas being primarily limited by fuel build-up and in mesic savannas by fuel moisture (Fig. 1, Krawchuk & Moritz, 2011; Kahiu & Hanan, 2018). In line with previous work, we find that fire activity in humid savannas and grasslands primarily responds to drought conditions during the fire season (Archibald *et al.*, 2010; Lehsten *et al.*, 2010; Alvarado *et al.*, 2017) similar to tropical rainforests (Aragão *et al.*,

2008). We find that fuel moisture was the dominant control on fire activity over 58.6% of tropical savannas and grasslands. These systems currently account for 59.1% of the tropical area burned, and the remaining 40.9% is in systems are fuel build-up limited.

Striking differences were observed across continents, with large areas of *fuel build-up limited* fire regimes occurring across more arid grasslands and savannas of southern Africa and northern Australia, and a near-absence of *fuel build-up limited* systems in tropical South America (Figs. 1 and 2). Fuel moisture formed the key control on burned area across South America's savannas, except for more arid grasslands along the eastern edge of the Brazilian Cerrado. Burned area in arid regions of Africa and Australia responded strongly to antecedent rainfall, highlighting the importance of fuel build-up and connectivity in these regions (Archibald *et al.*, 2010; Whitlock *et al.*, 2010; Krawchuk & Moritz, 2011; Price *et al.*, 2015). Continental scale differences were partly driven by differences in climate, for example, the extent of semi-arid and arid savannas with MAR<1000 mm yr-1 was largest across Africa and Australia, resulting in an overall larger fraction of ecosystems where fire occurrence was limited by *fuel build-up* (Fig. 1; Archibald *et al.*, 2010a). However, savanna fire regimes also switched from being dominantly *fuel build-up limited* to *fuel moisture limited* at different thresholds, around 500 mm yr^{-1} in South America, 800 mm yr^{-1} in Africa, and 1000 mm yr^{-1} in Australia (Fig. 2). Together, these two factors resulted in continental scale differences in fire regimes, and fire activity was limited by *fuel build-up* in only 24% of South American savannas, against 47% of African savannas and 61% of Australian savannas. Interestingly, these continental differences in fire regimes are in line with previous work showing similar differences in controls on savanna distribution and structure (Lehmann *et al.*, 2011, 2014). In the transition zones, where fire regimes switched from being predominantly *fuel-build up limited* to *fuel moisture limited*, the relationship between burned area and fuel dryness or fuel availability was often weak, and likely further modified by other climatic, ecological, and anthropogenic factors influencing fuel conditions.

4.2. Drivers of fire response

Seasonal rainfall distribution varied considerably across continents and had a strong effect on annual burned area (Fig. 3a). Previous analyses have shown that rainfall amount during the dry and wet seasons contribute to explain the spatial patterns of tropical fire activity (van der Werf *et al.*, 2008; Bowman *et al.*, 2014; Chen *et al.*, 2017), and that climate seasonality can explain observed differences in fire activity across regions with similar MAR (Saha *et al.*, 2019). We found that a minimum dry season duration of 6 to 8-months was required for

frequent fires to occur in productive and humid savannas, but we only detected a weak relationship between annual burned area and increasing dry season lengths longer than six months. A possible explanation for this weak relationship could be that dry season duration longer than six months may limit herbaceous productivity by shortening the growing season in spite of MAR. In addition, our results suggest that observed differences in rainfall seasonality may also modify the response of burned area to antecedent rainfall across different regions (Fig. 3b and c). Although the relatively long and pronounced African dry season is one of the factors contributing to high fire frequencies across the continent (Archibald *et al.*, 2009), African savannas were characterized by relatively low variability in burned area. In contrast, South American savannas were characterized by lower fire frequencies, but showed higher interannual variability in burned area driven by climate anomalies (cf. Figs. 3b and c; Alvarado *et al.*, 2017b; Chen *et al.*, 2017; Mataveli *et al.*, 2018).

Several analyses have shown that human land management, and therefore population density has a significant impact on global burned area (Bistinas *et al.*, 2013). In line with these findings, we found that higher human influence significantly reduced burned area across continents, with larger consequences for more densely populated continents like Africa and South America compared to Australia (Fig. 4a and Table A1; Archibald *et al.*, 2012; Andela *et al.*, 2017). Previous work has also shown that human land management may reduce the sensitivity of fire regimes to climate extremes (Bird et al., 2016). We found that the observed biogeographic differences in fire responses to antecedent rainfall could be related to human land management to some extent, but this factor alone could not explain the differences observed across continents (Fig. 4c). In general, areas with large annual mean burned area and low population densities, showed a relatively strong burned area response to rainfall variability. Nevertheless, this pattern did not hold everywhere, and particularly in savannas of intermediate productivity we observed an overall increase in the strength of the fuel-moisture effect on burned area in human dominated landscapes.

Continental scale differences in tree cover also explained part of the observed differences in fire-climate interactions. Previous work has shown that tree cover may limit fire activity in savannas (Archibald *et al.*, 2009), though these effects may be partly masked out in our study, that focuses on more open cover types with tree cover smaller or equal to 40%. Across areas with *fuel moisture limited* fire regimes, we observed a slight increase in the strength of the responses of BA to the antecedent rainfall with the increase of tree cover at similar MAR. While all three variables (DS, HII and TC) modified the response of burned area to antecedent

rainfall, none of these variables could explain the differences in thresholds observed across the continents (Figs. 3, 4 and 5). For example, when controlling for TC, continental scale differences in rainfall thresholds at which savannas switched from *fuel build-up* to *fuel moisture limited* fire regimes remained different.

To confirm these findings, we used a range of multiple linear regression models to explore if the continental scale differences could be explained by differences in DS, HII, and TC. Allowing the burned area to respond differently to antecedent rainfall across continents caused a considerable model improvement both when modeling absolute burned area (Table A1) or it's variability (Table 1). While the introduction of DS, HII and TC as additional explanatory variables further improved model performance, they only marginally affected continental scale differences in burned area response to antecedent rainfall (compare slopes in Table 1). Nevertheless, our linear model explained just 29% of absolute burned area and about 1% of the burned area anomalies even when considering continental scale differences in DS, HII and TC as additional drivers. Improving model representation of fire response to antecedent rainfall therefore remains a topic of future investigation. While we explored the role of dry season duration, it is possible that other indicators of vegetation and fuel conditions, like evapotranspiration, also play an important role (Boer et al. 2016). Similarly, regional differences in herbivory and human fire management, as well as the different composition and structure of grass and tree communities across continents may also be important (Lehmann et al., 2011).

Understanding the distribution of *fuel build-up* - and *fuel moisture limited* fire regimes is critical for fire management now and in the future, as changes in land management or climate may result in contrasting responses across *fuel* and *moisture limited* systems. In contrast to earlier studies that have suggested that fire activity in savannas was mostly limited by fuel availability (Whitlock *et al.*, 2010; Krawchuk & Moritz, 2011), we found that fuel moisture controlled burned area variability in more than half (58.6%) of the tropical savannas and grasslands, accounting for 59,1% of total burned area. Striking differences in burned area response to rainfall variability across continents highlighted that South American savannas were particularly sensitive to fuel moisture conditions, suggesting that rising temperatures may increase fire activity across the continent, and explaining the extraordinary strong response of fire activity across the continent to drought conditions driven by sea surface temperature anomalies (Chen et al., 2011). In contrast, a reduction of moisture availability would likely decrease burned area over most of Australia, where fire activity was mainly controlled by fuel build-up. In African savannas and grasslands, the area where burned area

was primarily controlled by fuel build-up was about equal to the area where fuel moisture conditions were most important. Although we could not conclusively attribute the continental scale differences to a single driver, we found that rainfall seasonality, human land management and tree cover all modified fire-climate interactions regionally through their effects on fuel availability and moisture status. Our work demonstrates that one single "global model" for savanna fires will not be enough to predict future fire regimes and fire regimes across different continents will likely respond differently to the same drivers of global change.

References

Abatzoglou, J.T., Williams, A.P., Boschetti, L., Zubkova, M. & Kolden, C.A. (2018) Global patterns of interannual climate-fire relationships. *Global Change Biology*, **24**, 5164–5175.

Aleman, J.C. & Staver, A.C. (2018) Spatial patterns in the global distributions of savanna and forest. *Global Ecology and Biogeography*, **27**, 792–803.

Alvarado, S.T., Fornazari, T., Cóstola, A., Morellato, L.P.C. & Silva, T.S.F. (2017) Drivers of fire occurrence in a mountainous Brazilian cerrado savanna: Tracking long-term fire regimes using remote sensing. *Ecological Indicators*, **78**, 270–281.

Andela, N., Morton, D.C., Giglio, L., Chen, Y., van der Werf, G.R., Kasibhatla, P.S., DeFries, R.S., Collatz, G.J., Hantson, S., Kloster, S., Bachelet, D., Forrest, M., Lasslop, G., Li, F., Mangeon, S., Melton, J.R., Yue, C. & Randerson, J.T. (2017) A human-driven decline in global burned area. *Science*, **356**, 1356–1362.

Aragão, L.E.O.C., Malhi, Y., Barbier, N., Lima, A., Shimabukuro, Y., Anderson, L. & Saatchi, S. (2008) Interactions between rainfall, deforestation and fires during recent years in the Brazilian Amazonia. *Philosophical Transactions of the Royal Society B: Biological Sciences*, **363**, 1779–1785.

Archibald, S., Nickless, A., Govender, N., Scholes, R.J. & Lehsten, V. (2010) Climate and the inter-annual variability of fire in southern Africa: a meta-analysis using long-term field data and satellite-derived burnt area data. *Global Ecology and Biogeography*, **19**, 794–809.

Archibald, S., Roy, D.P.D., Wilgen, V., Brian, W. & Scholes, R.J. (2009) What limits fire? An examination of drivers of burnt area in Southern Africa. *Global Change Biology*, **15**, 613–630.

Archibald, S., Staver, A.C. & Levin, S.A. (2012) Evolution of human-driven fire regimes in Africa. *Proceedings of the National Academy of Sciences*, **109**, 847–852.

Benali, A., Mota, B., Carvalhais, N., Oom, D., Miller, L.M., Campagnolo, M.L. & Pereira, J.M.C. (2017) Bimodal fire regimes unveil a global-scale anthropogenic fingerprint. *Global Ecology and Biogeography*, **26**, 799–811.

Bird, R.B., Bird, D.W. & Codding, B.F. (2016) People, El Niño southern oscillation and fire in Australia: fire regimes and climate controls in hummock grasslands. *Philosophical transactions of the Royal Society of London. Series B, Biological sciences*, **371**, 20150343.

Bird, R.B., Codding, B.F., Kauhanen, P.G. & Bird, D.W. (2012) Aboriginal hunting buffers climate-driven fire-size variability in Australia's spinifex grasslands. *Proceedings of the National Academy of Sciences of the United States of America*, **109**, 10287–10292.

Bistinas, I., Harrison, S.P., Prentice, I.C. & Pereira, J.M.C. (2014) Causal relationships versus emergent patterns in the global controls of fire frequency. *Biogeosciences*, **11**, 5087–5101.

Bistinas, I., Oom, D., Sá, A.C.L., Harrison, S.P., Prentice, I.C. & Pereira, J.M.C. (2013) Relationships between Human Population Density and Burned Area at Continental and Global Scales. *PLoS ONE*, **8**, e81188.

Boer, M.M., Bowman, D.M.J.S., Murphy, B.P., Cary, G.J., Cochrane, M.A., Fensham, R.J., Krawchuk, M.A., Price, O.F., De Dios, V.R., Williams, R.J. & Bradstock, R.A. (2016) Future changes in climatic water balance determine potential for transformational shifts in Australian fire regimes. *Environmental Research Letters*, **11**, 065002.

Bond, W.J., Woodward, F.I. & Midgley, G.F. (2005) The global distribution of ecosystems in a world without fire. *New Phytologist*, **165**, 525–538.

Bowman, D.M.J.S., Balch, J., Artaxo, P., Bond, W.J., Cochrane, M.A., D'Antonio, C.M., DeFries, R., Johnston, F.H., Keeley, J.E., Krawchuk, M.A., Kull, C.A., Mack, M., Moritz, M.A., Pyne, S., Roos, C.I., Scott, A.C., Sodhi, N.S. & Swetnam, T.W. (2011) The human dimension of fire regimes on Earth. *Journal of Biogeography*, **38**, 2223–2236.

Bowman, D.M.J.S., Murphy, B.P., Williamson, G.J. & Cochrane, M.A. (2014) Pyrogeographic models, feedbacks and the future of global fire regimes. *Global Ecology and Biogeography*, **23**, 821–824.

Bradstock, R.A. (2010) A biogeographic model of fire regimes in Australia: current and future implications. *Global Ecology and Biogeography*, **19**, 145–158.

Burnham, K.P. & Anderson, D.R. (2004) Multimodel Inference Understanding AIC and BIC in Model Selection. *Sociological Methods & Research*, **33**, 261–304.

Chen, Y., Morton, D.C., Andela, N., van der Werf, G.R., Giglio, L. & Randerson, J.T. (2017) A pan-tropical cascade of fire driven by El Niño/Southern Oscillation. *Nature Climate Change*, **7**, 906–911.

Chen, Y., Randerson, J., Morton, D., DeFries, R., Collatz, G., Kasibhatla, P., Giglio, L., Jin, Y. & Marlier, M. (2011) Forecasting fire season severity in South America using sea surface temperature anomalies. *Science*, **334**, 787–791.

Chuvieco, E., Giglio, L. & Justice, C. (2008) Global characterization of fire activity: toward defining fire regimes from Earth observation data. *Global Change Biology*, **14**, 1488–1502.

Cochrane, M.A. & Ryan, K.C. (2009) *Fire and fire ecology: Concepts and principles*. Springer Praxis Books., pp. 25–62. Springer Berlin Heidelberg.

Daniau, A.-L., Bartlein, P.J., Harrison, S.P., Prentice, I.C., Brewer, S., Friedlingstein, P., Harrison-Prentice, T.I., Inoue, J., Izumi, K., Marlon, J.R., Mooney, S., Power, M.J., Stevenson, J., Tinner, W., Andrič, M., Atanassova, J., Behling, H., Black, M., Blarquez, O., Brown, K.J., Carcaillet, C., Colhoun, E.A., Colombaroli, D., Davis, B.A.S., D'Costa, D., Dodson, J., Dupont, L., Eshetu, Z., Gavin, D.G., Genries, A., Haberle, S., Hallett, D.J., Hope, G., Horn, S.P., Kassa, T.G., Katamura, F., Kennedy, L.M., Kershaw, P., Krivonogov, S., Long, C., Magri, D., Marinova, E., McKenzie, G.M., Moreno, P.I., Moss, P., Neumann, F.H., Norström, E., Paitre, C., Rius, D., Roberts, N., Robinson, G.S., Sasaki, N., Scott, L., Takahara, H., Terwilliger, V., Thevenon, F., Turner, R., Valsecchi, V.G., Vannière, B., Walsh, M., Williams, N. & Zhang, Y. (2012) Predictability of biomass burning in response to climate changes. *Global Biogeochemical Cycles*, **26**, GB4007.

DiMiceli, C.M., Carroll, M.L., Sohlberg, R.A., Huang, C., Hansen, M.C. & Townshend, J.R.G. (2011) *Annual Global Automated MODIS Vegetation Continuous Fields (MOD44B) at 250 m Spatial Resolution for Data Years Beginning Day 65, 2000 - 2010, Collection 5 Percent Tree Cover*, University of Maryland, College Park, MD, USA.

Forkel, M., Dorigo, W., Lasslop, G., Teubner, I., Chuvieco, E. & Thonicke, K. (2017) A data-driven approach to identify controls on global fire activity from satellite and climate observations (SOFIA V1). *Geoscientific Model Development*, **10**, 4443–4476.

Friedl, M.A., Sulla-Menashe, D., Tan, B., Schneider, A., Ramankutty, N., Sibley, A. & Huang, X. (2010) MODIS Collection 5 global land cover: Algorithm refinements and characterization of new datasets. *Remote Sensing of Environment*, **114**, 168–182.

Funk, C., Peterson, P., Landsfeld, M., Pedreros, D., Verdin, J., Shukla, S., Husak, G., Rowland, J., Harrison, L., Hoell, A. & Michaelsen, J. (2015) The climate hazards infrared precipitation with stations—a new environmental record for monitoring extremes. *Scientific Data*, **2**, 150066.

Giglio, L., Boschetti, L., Roy, D.P., Humber, M.L. & Justice, C.O. (2018) The Collection 6 MODIS burned area mapping algorithm and product. *Remote Sensing of Environment*, **217**, 72–85.

Hantson, S., Arneth, A., Harrison, S.P., Kelley, D.I., Prentice, I.C., Rabin, S.S., Archibald, S., Mouillot, F., Arnold, S.R., Artaxo, P., Bachelet, D., Ciais, P., Forrest, M., Friedlingstein, P., Hickler, T., Kaplan, J.O., Kloster, S., Knorr, W., Lasslop, G., Li, F., Mangeon, S., Melton, J.R., Meyn, A., Sitch, S., Spessa, A., van der Werf, G.R., Voulgarakis, A. & Yue, C. (2016) The status and challenge of global fire modelling. **13**, 3359–3375.

Hantson, S., Scheffer, M., Pueyo, S., Xu, C., Lasslop, G., van Nes, E.H., Holmgren, M. & Mendelsohn, J. (2017) Rare, Intense, Big fires dominate the global tropics under drier conditions. *Scientific Reports*, **7**, 14374.

Hoffmann, W.A., Geiger, E.L., Gotsch, S.G., Rossatto, D.R., Silva, L.C.R., Lau, O.L., Haridasan, M. & Franco, A.C. (2012) Ecological thresholds at the savanna-forest boundary: how plant traits, resources and fire govern the distribution of tropical biomes. *Ecology Letters*, **15**, 759–768.

Hulme, M. & Viner, D. (1998) *A Climate Change Scenario for the Tropics*. *Potential Impacts of Climate Change on Tropical Forest Ecosystems*, pp. 5–36. Springer Netherlands, Dordrecht.

Jolly, W.M., Cochrane, M.A., Freeborn, P.H., Holden, Z.A., Brown, T.J., Williamson, G.J. & Bowman, D.M.J.S. (2015) Climate-induced variations in global wildfire danger from 1979 to 2013. *Nature Communications*, **6**, 7537.

Kahiu, M.N. & Hanan, N.P. (2018) Fire in sub-Saharan Africa: The fuel, cure and connectivity hypothesis. *Global Ecology and Biogeography*, **27**, 946–957.

Krawchuk, M.A. & Moritz, M.A. (2011) Constraints on global fire activity vary across a resource gradient. *Ecology*, **92**, 121–132.

Lasslop, G., Moeller, T., D'Onofrio, D., Hantson, S. & Kloster, S. (2018) Tropical climate–vegetation–fire relationships: multivariate evaluation of the land surface model JSBACH. *Biogeosciences*, **15**, 5969–5989.

Lehmann, C.E., Anderson, T.M., Sankaran, M., Higgins, S.I., Archibald, S., Hoffmann, W.A., Hanan, N.P., Williams, R.J., Fensham, R.J., Felfili, J. & others (2014) Savanna vegetation-fire-climate relationships differ among continents. *Science*, **343**, 548–552.

Lehmann, C.E.R., Archibald, S.A., Hoffmann, W.A. & Bond, W.J. (2011) Deciphering the distribution of the savanna biome. *New Phytologist*, **191**, 197–209.

Lehsten, V., Harmand, P., Palumbo, I. & Arneth, A. (2010) Modelling burned area in Africa. *Biogeosciences*, **7**, 3199–3214.

van Marle, M.J.E., Kloster, S., Magi, B.I., Marlon, J.R., Daniau, A.-L., Field, R.D., Arneth, A., Forrest, M., Hantson, S., Kehrwald, N.M., Knorr, W., Lasslop, G., Li, F., Mangeon, S., Yue, C., Kaiser, J.W. & van der Werf, G.R. (2017) Historic global biomass burning emissions based on merging satellite observations with proxies and fire models (1750–2015). *Geoscientific Model Development Discussions*, **10**, 3329–3357.

Mataveli, G.A.V., Silva, M.E.S., Pereira, G., Cardozo, F.D.S., Kawakubo, F.S., Bertani, G., Costa, J.C., Ramos, R.D.C. & Silva, V.V. Da (2018) Satellite observations for describing fire patterns and climate-related fire drivers in the Brazilian savannas. *Hazards Earth Syst. Sci*, **18**, 125–144.

Mistry, J. (2000) *World savannas: ecology and human use*, Prentice Hall (a Pearson Education Company).

Moritz, M.A., Parisien, M.-A., Batllori, E., Krawchuk, M.A., Van Dorn, J., Ganz, D.J. & Hayhoe, K. (2012) Climate change and disruptions to global fire activity. *Ecosphere*, **3**, 1–22.

Morton, D.C., DeFries, R.S., Nagol, J., Souza, C.M., Kasischke, E.S., Hurtt, G.C. & Dubayah, R. (2011) Mapping canopy damage from understory fires in Amazon forests using annual time series of Landsat and MODIS data. *Remote Sensing of Environment*, **115**, 1706–1720.

O'Donnell, A.J., Boer, M.M., McCaw, W.L. & Grierson, P.F. (2011) Vegetation and landscape connectivity control wildfire intervals in unmanaged semi-arid shrublands and woodlands in Australia. *Journal of Biogeography*, **38**, 112–124.

Le Page, Y., Oom, D., Silva, J.M.N., Jönsson, P. & Pereira, J.M.C. (2010) Seasonality of vegetation fires as modified by human action: observing the deviation from eco-climatic fire regimes. *Global Ecology and Biogeography*, **19**, 575–588.

Pausas, J.G. & Paula, S. (2012) Fuel shapes the fire–climate relationship: evidence from Mediterranean ecosystems. *Global Ecology and Biogeography*, **21**, 1074–1082.

Pausas, J.G. & Ribeiro, E. (2013) The global fire–productivity relationship. *Global Ecology and Biogeography*, **22**, 728–736.

Price, O.F., Pausas, J.G., Govender, N., Flannigan, M., Fernandes, P.M., Brooks, M.L. & Bird, R.B. (2015) Global patterns in fire leverage: The response of annual area burnt to previous fire. *International Journal of Wildland Fire*, **24**, 297–306.

Price, O.F., Russell-Smith, J. & Watt, F. (2012) The influence of prescribed fire on the extent of wildfire in savanna landscapes of western Arnhem Land, Australia. *International Journal of Wildland Fire*, **21**, 297–305.

R Core Team (2016) R: A language and environment for statistical computing. R Foundation for Statistical Computing.

Rabin, S.S., Melton, J.R., Lasslop, G., Bachelet, D., Forrest, M., Hantson, S., Kaplan, J.O., Li, F., Mangeon, S., Ward, D.S., Yue, C., Arora, V.K., Hickler, T., Kloster, S., Knorr, W., Nieradzik, L., Spessa, A., Folberth, G.A., Sheehan, T., Voulgarakis, A., Kelley, D.I., Prentice, I.C., Sitch, S., Harrison, S. & Arneth, A. (2017) The Fire Modeling Intercomparison Project (FireMIP), phase 1: experimental and analytical protocols with detailed model descriptions. *Geoscientific Model Development*, **10**, 1175–1197.

Ratnam, J., Tomlinson, K.W., Rasquinha, D.N. & Sankaran, M. (2016) Savannahs of Asia: antiquity, biogeography, and an uncertain future. *Philosophical transactions of the Royal Society of London. Series B, Biological sciences*, **371**, 20150305.

Saha, M. V., Scanlon, T.M. & D'Odorico, P. (2019) Climate seasonality as an essential predictor of global fire activity. *Global Ecology and Biogeography*, **28**, 198–210.

Voulgarakis, A. & Field, R.D. (2015) Fire Influences on Atmospheric Composition, Air Quality and Climate. *Current Pollution Reports*, **1**, 70–81.

WCS, W.C.S.- & University, C. for I.E.S.I.N.-C.-C. (2005) Last of the Wild Project, Version 2, 2005 (LWP-2): Global Human Influence Index (HII) Dataset (Geographic).

van der Werf, G.R., Randerson, J.T., Giglio, L., Gobron, N. & Dolman, A.J. (2008) Climate controls on the variability of fires in the tropics and subtropics. *Global Biogeochemical Cycles*, **22**, GB3028.

Whitlock, C., Higuera, P.E., McWethy, D.B. & Briles, C.E. (2010) Paleoecological perspectives on fire ecology: revisiting the fire-regime concept. *Open Ecology Journal*, **3**, 6–23.

Van Wilgen, B.W., Govender, N., Biggs, H.C., Ntsala, D. & Funda, X.N. (2004) Response of Savanna Fire Regimes to Changing Fire-Management Policies in a Large African National Park. *Conservation Biology*, **18**, 1533–1540.

Williams, A.P. & Abatzoglou, J.T. (2016) Recent Advances and Remaining Uncertainties in Resolving Past and Future Climate Effects on Global Fire Activity. *Current Climate Change Reports*, **2**, 1–14.

Yibarbuk, D., Whitehead, P.J., Russell-Smith, J., Jackson, D., Godjuwa, C., Fisher, A., Cooke, P., Choquenot, D. & Bowman, D.M.J.S. (2002) Fire ecology and Aboriginal land management in central Arnhem Land, northern Australia: a tradition of ecosystem management. *Journal of Biogeography*, **28**, 325–343.

Data Accessibility:

Biome wide gridded raster layers (GeoTIFF) of mean annual rainfall, tree cover, dry season duration, and human development index, as well as per fire-year burned area and antecedent rainfall (6 and 24-month accumulation periods) along with inferred maps of fire-response to antecedent rainfall are available on Zenodo web site (https://zenodo.org/)

Tables

Table 1. Multiple Linear Regression Models explaining the variation of annual burned area anomalies ($BA_{i,j}$ *anomaly*) in pixel *i* and year *j* for tropical savannas and grasslands areas (2002 – 2016). The variables representing the fuel moisture effect (6 months of accumulated rainfall; $Rain6_{i,j}$), and the fuel build-up effect (24 months of accumulated rainfall; $Rain24_{i,j}$), varied both by pixel *i* and year *j*. Other variables, including mean annual rainfall (MAR_i), dry season duration (DS_i), human influence index (HII_i) and tree cover (TC_i) varied by pixel *i* only. Model performance was evaluated based on the coefficient of determination (R^2), p-value and Akaike's Information Criterion (AIC). All models were significant at $p<0.001$.

Regression model	**Regression equation**	**R^2**	**AIC**
$Rain6_{i,j} + Rain24_{i,j}$	$BA_{i,j}$ anomaly ~ -0.22 – 0.0018 * $Rain6_{i,j}$ + 0.00040 * $Rain24_{i,j}$ + εij	0.0019	2090280
$Rain6_{i,j} : MAR_i + Rain24_{i,j} : MAR_i$	$BA_{i,j}$ anomaly ~ 0.0098 – 0.0000011 * $Rain6_{i,j} : MAR_i$ + 0.00000018 * $Rain24_{i,j} : MAR_i$ + εij	0.0013	2090422
$Rain6_{i,j} : Continent_i + Rain24_{i,j} : Continent_i$	$BA_{i,j}$ anomaly ~ -0.43 – 0.0011 * $Rain6_{i,j} : Africa_i$ – 0.0037 * $Rain6_{i,j} : Australia_i$ – 0.0033 * $Rain6_{i,j} : SouthAmerica_i$ + 0.00041 * $Rain24_{i,j} : Africa_i$ + 0.00088 * $Rain24_{i,j} : Australia_i$ + 0.00058 * $Rain24_{i,j} : SouthAmerica_i$ + εij	0.0029	2089998
$Rain6_{i,j} : Continent_i + Rain24_{i,j} : Continent_i + DS_i : Continent$	$BA_{i,j}$ anomaly ~ 0.38 – 0.0012 * $Rain6_{i,j} : Africa_i$ – 0.0034 * $Rain6_{i,j} : Australia_i$ – 0.0035 * $Rain6_{i,j} : SouthAmerica_i$ + 0.00023 * $Rain24_{i,j} : Africa_i$ + 0.0014 * $Rain24_{i,j} : Australia_i$ + 0.00051* $Rain24_{i,j} : SouthAmerica_i$ – 0.062 * $DS_i : Africa_i$ – 0.31 * $DS_i : Australia_i$ – 0.12 * $DS_i : SouthAmerica_i$ + εij	0.0034	2089875
$Rain6_{i,j} : Continent_i + Rain24_{i,j} : Continent_i + HII_i : Continent_i$	$BA_{i,j}$ anomaly ~ -0.55 – 0.0011 * $Rain6_{i,j} : Africa_i$ – 0.0036 * $Rain6_{i,j} : Australia_i$ – 0.0033 * $Rain6_{i,j} : SouthAmerica_i$ + 0.00040 * $Rain24_{i,j} : Africa_i$ + 0.0011 * $Rain24_{i,j} : Australia_i$ + 0.00054 * $Rain24_{i,j} : SouthAmerica_i$ + 0.011 * $HII_i : Africa_i$ – 0.11 * $HII_i : Australia_i$ + 0.017 * $HII_i : SouthAmerica_i$ + εij	0.0031	2089957
$Rain6_{i,j} : Continent_i + Rain24_{i,j} : Continent_i + TC_i : Continent_i$	$BA_{i,j}$ anomaly ~ -0.42 – 0.0012 * $Rain6_{i,j} : Africa_i$ – 0.0038 * $Rain6_{i,j} : Australia_i$ – 0.0033 * $Rain6_{i,j} : SouthAmerica_i$ + 0.00049 * $Rain24_{i,j} : Africa_i$ + 0.0015 * $Rain24_{i,j} : Australia_i$ + 0.00050 * $Rain24_{i,j} : SouthAmerica_i$ – 0.010 * $TC_i : Africa_i$ – 0.13 * $TC_i : Australia_i$ + 0.010 * $TC_i : SouthAmerica_i$ + εij	0.0034	2089868
$Rain6_{i,j} : Continent_i + Rain24_{i,j} : Continent_i + TC_i : Continent_i + DS_i : Continent_i + HII_i : Continent_i$	$BA_{i,j}$ anomaly ~ 0.36 – 0.0012 * $Rain6_{i,j} : Africa_i$ – 0.0036 * $Rain6_{i,j} : Australia_i$ – 0.0036 * $Rain6_{i,j} : SouthAmerica_i$ + 0.00035 * $Rain24_{i,j} : Africa_i$ + 0.0019 * $Rain24_{i,j} : Australia_i$ + 0.00046 * $Rain24_{i,j} : SouthAmerica_i$ – 0.013 * $TC_i : Africa_i$ – 0.13 * $TC_i : Australia_i$ + 0.0077 * $TC_i : SouthAmerica_i$ – 0.055 * $DS_i : Africa_i$ – 0.29 * $DS_i : Australia_i$ – 0.16 * $DS_i : SouthAmerica_i$ – 0.0064 * $HII_i : Africa_i$ + 0.058 * $HII_i : Australia_i$ + 0.016 * $HII_i : SouthAmerica_i$ + εij	0.0039	2089756

661 **Figures**

662

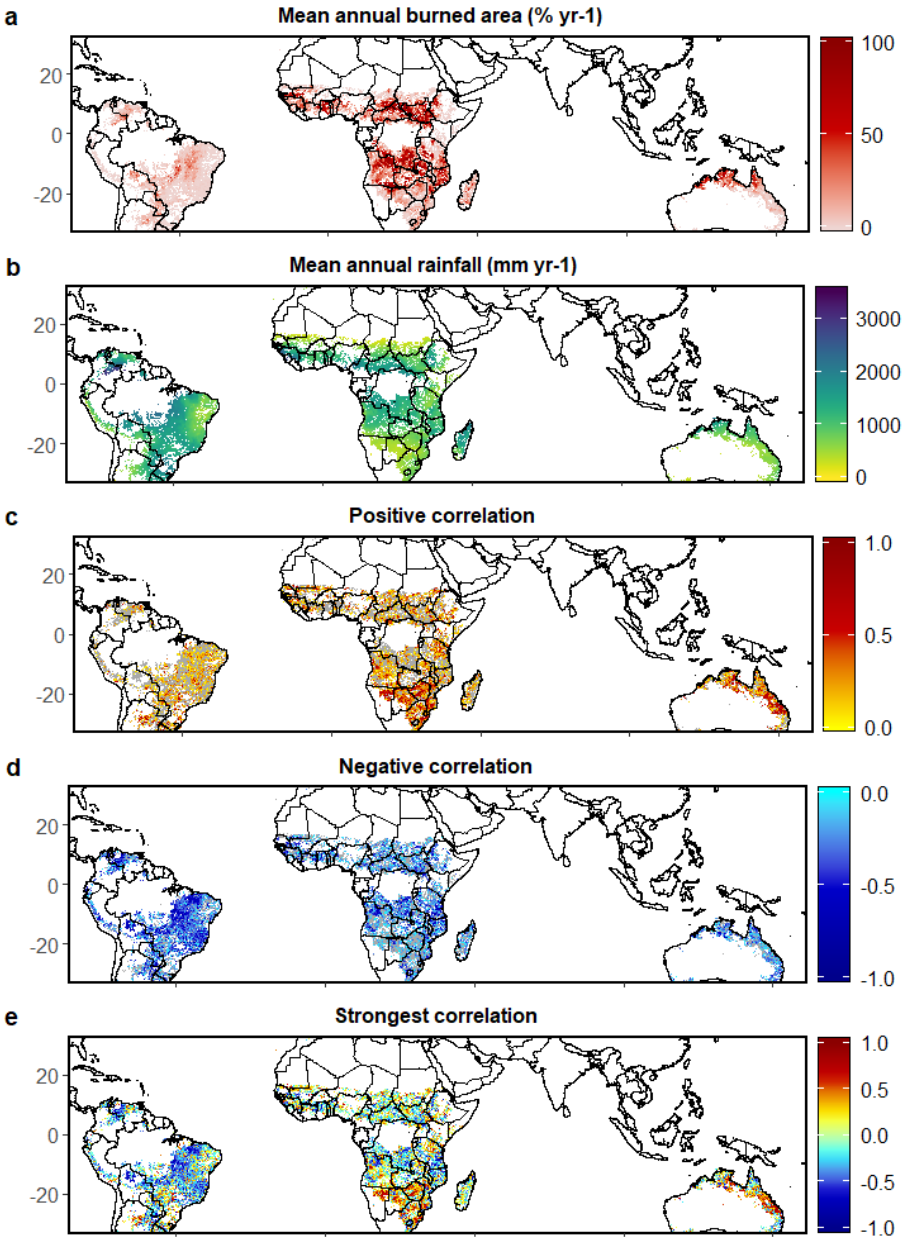

663

664

665 **Fig. 1.** Rainfall – burned area interactions varied widely across continents. (a) Mean annual
666 burned area (% yr^{-1}), (b) mean annual rainfall (mm yr-1), (c) correlation between annual
667 burned area and 24 months of antecedent rainfall (positive correlations), (d) correlation
668 between annual burned area and 6 months of antecedent rainfall (negative correlations), and
669 (e) the strongest absolute correlation shown in (c and d). Figure e shows the distribution of
670 *fuel build-up limited* (positive correlation) and *fuel moisture limited* (negative correlation) fire
671 regimes across tropical savannas. Grid cells with land cover classes other than savannas and
672 grasslands were excluded from our analysis and are masked in white. Pixels with negative
673 correlations in b and positive correlations in c were masked in grey.

674

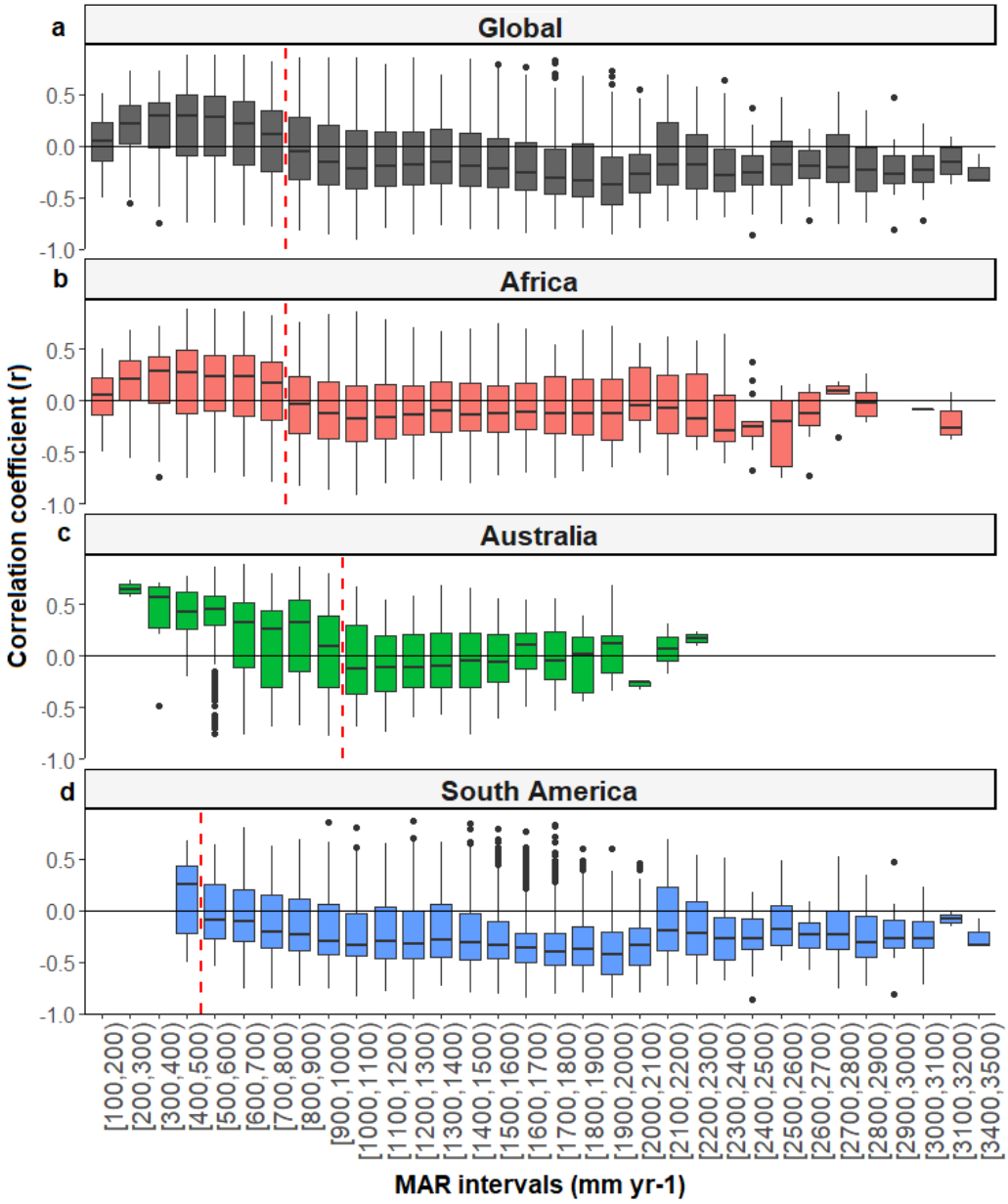

Fig. 2. Box-and-whisker plots of the response of burned area to antecedent rainfall. Results for (a) Pantropical savannas and grasslands, and for (b) Africa, (c) Australia, and (d) South America, separately. Box plots include all 0.25° grid cells per bin of 100 mm mean annual rainfall (MAR). For each grid cell we registered a single response (positive, based on 24-months of antecedent precipitation) or negative (based on 6 months of antecedent rainfall) using the per-grid cell strongest absolute correlation. The boxes indicate the 25th and 75th percentile of the data, the mid band indicates the median, and the whiskers indicate the 5th and 95th percentiles. Box plots with less than 5 pixels were excluded from this figure.

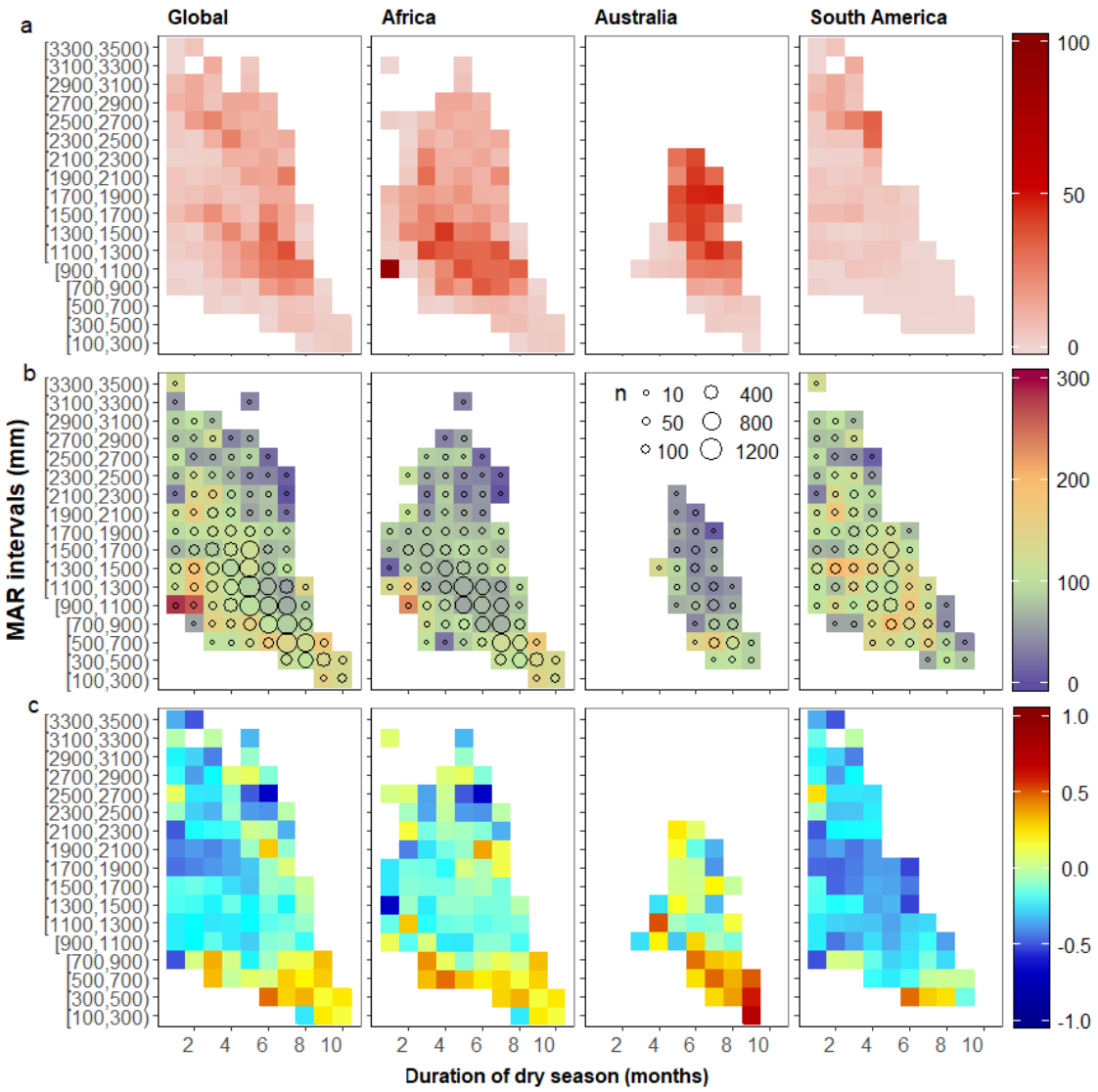

Fig. 3. Burned area response to dry season duration. (a) Median burned area (% yr^{-1}) per bin of Mean Annual Rainfall (MAR intervals) and dry season duration (b) Coefficient of variation of burned area per bin of Mean Annual Rainfall and dry season duration, circle size represent the upper limit of the number of grid cells by bin (*n* = number of grid cells). (c) Median correlation coefficient based on the per-pixel strongest absolute correlation within each bin of Mean Annual Rainfall and dry season duration. Cells with less than 3 pixels were excluded from panel b because the coefficients of variation calculate require at least 3 data.

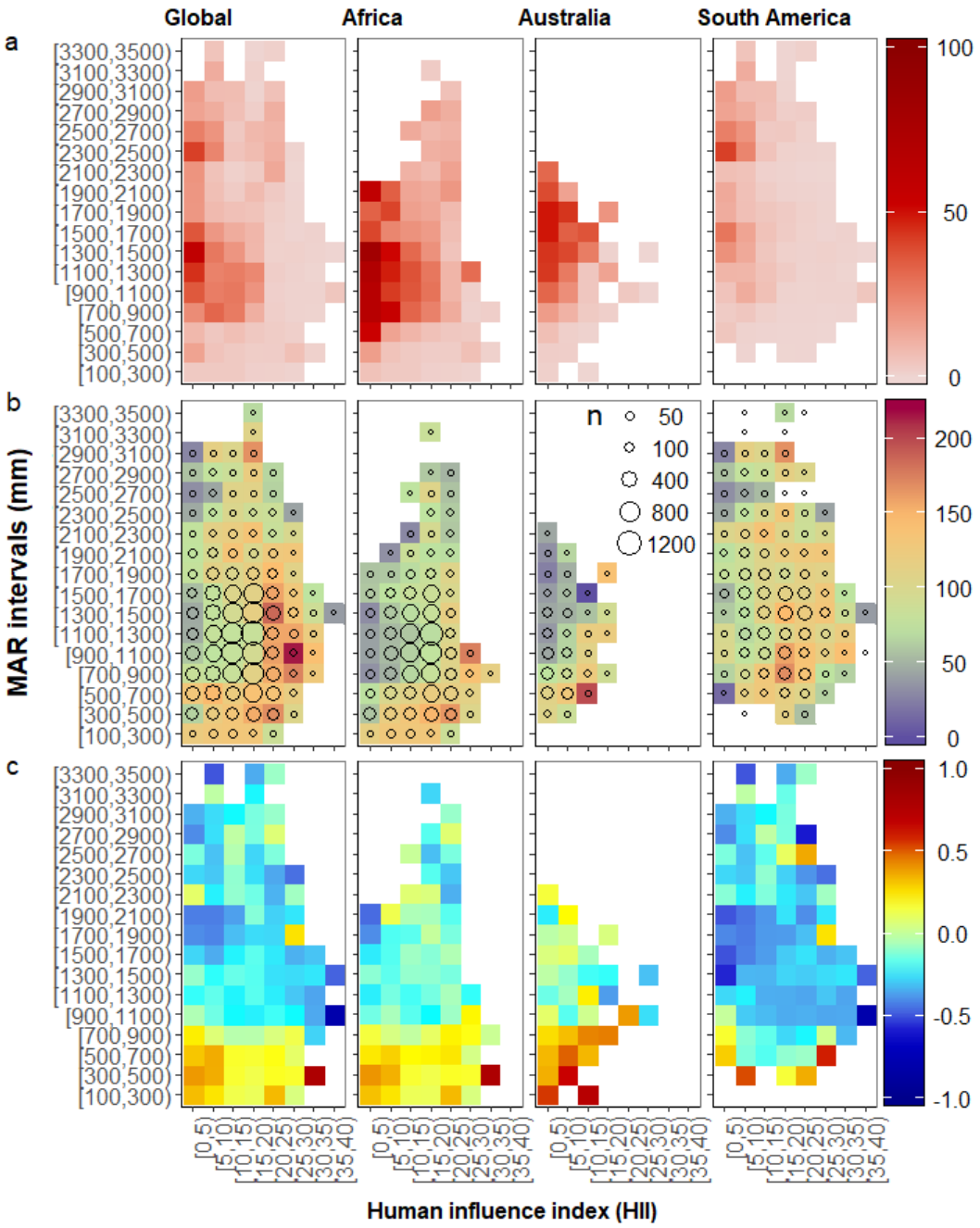

Fig. 4. Burned Area response to human land management. (a) Median burned area (% yr^{-1}) per bin of Mean Annual Rainfall (MAR intervals) and Human influence index. (b) Coefficient of variation of burned area per bin of Mean Annual Rainfall and Human influence index, circle size represent the upper limit of the number of grid cells by bin (*n* = number of grid cells). (c) Median correlation coefficient, based on the per-pixel strongest absolute correlation within each bin of Mean Annual Rainfall and Human influence index. Cells with less than 3 pixels were excluded from panel b because the coefficients of variation calculate require at least 3 data.

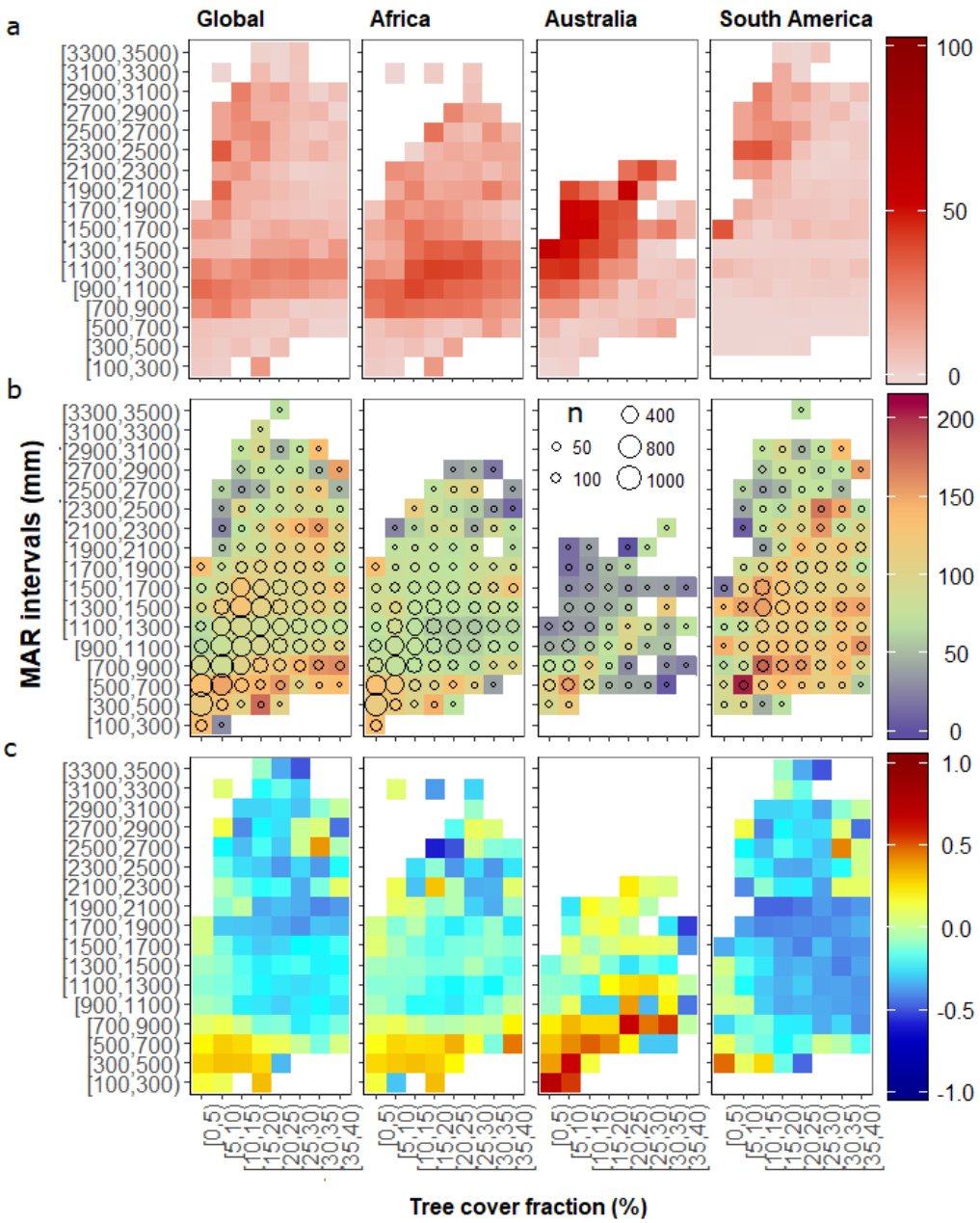

Fig. 5. Burned Area response to tree cover fraction. (a) Median burned area (% yr^{-1}) per bin of Mean Annual Rainfall (MAR intervals) and tree cover fraction (%). (b) Coefficient of variation of burned area per bin of Mean Annual Rainfall and tree cover fraction, circle size represent the upper limit of the number of grid cells by bin (*n* = number of grid cells). (c) Median correlation coefficient, based on the per-pixel strongest absolute correlation within each bin of Mean Annual Rainfall and tree cover fraction. Cells with less than 3 pixels were excluded from panel b because the coefficients of variation calculate require at least 3 data.